



Coupling diffusion and maximum entropy models to estimate thermal inertia

Grey S. Nearing^{a,*}, M. Susan Moran^b, Russell L. Scott^b, Guillermo Ponce-Campos^b

^a University of Arizona, Hydrology and Water Resources Department, Tucson, AZ, United States

^b USDA-ARS Southwest Watershed Research Center, Tucson, AZ, United States

ARTICLE INFO

Article history:

Received 12 August 2011

Received in revised form 15 December 2011

Accepted 17 December 2011

Available online 26 January 2012

Keywords:

Thermal inertia

Surface energy balance

Maximum entropy production

Soil moisture

ABSTRACT

Thermal inertia is a physical property of soil at the land surface related to water content. We developed a method for estimating soil thermal inertia using two daily measurements of surface temperature, to capture the diurnal range, and diurnal time series of net radiation and specific humidity. The method solves for soil thermal inertia assuming homogeneous 1-D diffusion of heat near the land surface. The solution uses a boundary condition taken as the maximum likelihood estimate of ground heat flux made by a probabilistic uncertainty model of the partitioning of net radiation based on the theory of maximum entropy production (MEP model). We showed that by coupling the 1-D diffusion and MEP models of energy transfer at the land surface, the number of free parameters in the MEP model can be reduced from two (P – soil thermal inertia and I – thermal inertia of convective heat transfer to the atmosphere) to one (P is defined by I). A sensitivity analysis suggested that, for the purpose of estimating thermal inertia, the coupled model should be parameterized by the ratio P/I . The coupled model was demonstrated at two semi-arid sites in the southwest United States to estimate thermal inertia and these thermal inertia values were used to estimate soil moisture. We found 1) parameterizing the MEP model with a constant annual P/I value resulted in surface flux estimates which were similar to those made when daily P and I parameters were derived directly from measurements of ground heat flux (Nash-Sutcliffe efficiency > 0.95); 2) estimates of P made using the coupled model were superior to those made using the diffusion model with a common linear approximation of the ground heat flux boundary condition; and 3) thermal inertia was a better predictor of soil moisture in moderately wet conditions than in dry conditions due to a lack of sensitivity of thermal inertia to changes in soil moisture at low moisture contents.

© 2012 Elsevier Inc. All rights reserved.

1. Introduction

Thermal inertia, P [$\text{Jm}^{-2} \text{s}^{-1/2} \text{K}^{-1}$], is a physical property of the land surface which determines resistance to temperature change under seasonal or diurnal heating. It is a function of volumetric heat capacity, c [$\text{Jm}^{-3} \text{K}^{-1}$], and thermal conductivity, k [$\text{Wm}^{-1} \text{K}^{-1}$] of the soil or other geologic material near the surface:

$$P = \sqrt{ck}. \quad (1)$$

Thermal inertia of soil varies with moisture content due the difference between thermal properties of water ($c_w \approx 4.18$, $k_w \approx 0.59$) and air (dry: $c_a \approx 0.0013$, $k_a \approx 0.25$). The temperature of a wet soil varies less with diurnal heating than the temperature of a dry soil and a number of studies have demonstrated that it is feasible to estimate soil moisture given thermal inertia (e.g. Lu et al., 2009; Price, 1980).

* Corresponding author at: University of Arizona, Department of Hydrology and Water Resources, 1133 E James E. Rogers Way, Harshbarger Bldg, Room 122, Tucson, AZ 85721, United States. Tel.: +1 520 269 1774; fax: +1 520 626 9712.

E-mail address: grey@email.arizona.edu (G.S. Nearing).

The problem of estimating thermal inertia using measurements of surface temperature, perhaps in conjunction with other observations, has also been widely studied; van de Griend et al. (1985) gave a concise contemporary review and Cracknell and Xue (1996a) summarized further developments. The common approach for estimating thermal inertia is to model the Earth's surface as a 1-dimensional homogeneous diffusive half-space and derive surface temperature as a function of the ground heat flux (G) boundary condition and soil thermal properties. Cracknell and Xue (1996b) describe a classical Fourier solution to the 1-D diffusion equation which can be used to estimate a daily value of thermal inertia from two observations of surface temperature and a time series of ground heat flux measurements. The primary issue in applying this technique is that it is difficult to obtain continuous measurements of G , and a number of studies have tried to accommodate for this. For instance, Verhoef (2004) used the nighttime drop in surface temperature and an assumption that during the night, ground heat flux is equal to net radiation, and found that this led to reasonable estimates of P on clear, windstill nights. Wang et al. (2010) approximated a diffusion solution using the diurnal amplitude of ground heat flux in a way which required only two daily measurements of G . Xue and Cracknell (1995) derived a solution for P by approximating the ground heat flux boundary condition as a linear

function of surface temperature according to Watson (1975). This required a time series of surface-incident radiation and an estimate of the phase shift between one of the harmonic functions of surface radiation and the same harmonic of surface temperature. When there were no clouds and surface radiation could be approximated as a sine curve, this was estimated as the time difference between maximum temperature and maximum radiation and only two measurements of surface temperature were necessary to derive a daily P value. When there are clouds, time series of both surface radiation and surface temperature are needed to estimate this phase shift.

Recently, Wang and Bras (2011) developed a method for partitioning net radiation into sensible, ground and latent heat fluxes based on the principle of maximum entropy production (Dewar, 2005). This method (referred to as MEP) requires two parameters: thermal inertia of the soil and a thermal inertia-like parameter representing resistance of the atmosphere to turbulent heat convection. It was derived as a probabilistic minimization of epistemic uncertainty and differs conceptually from the physically-based diffusion approach to linking ground heat flux and soil thermal inertia.

In this paper, we combine the diffusion and MEP models for the purpose of estimating daily values of soil thermal inertia. The result is a reduction in the number of parameters required for MEP partitioning of surface fluxes from two to one. The model requires only a single (daily) parameter and inputs in the form of a net radiation time series and two daily measurements of surface temperature. We show that this coupling results in an approximation of a diffusion-like representation of near-surface turbulent convection, and we chose an appropriate parameterization of the coupled model for the purpose of estimating P based on a sensitivity analysis. The ability of the model to estimate soil thermal inertia was demonstrated using measurements taken at a field site in southern Arizona, USA, and an example of estimating soil moisture from thermal inertia is provided. Finally, we provide a demonstration of the method for estimating thermal inertia using level 3 MODIS imagery taken by the Aqua platform in 2004.

2. Model development

2.1. The diffusion model

Heat flow in a one dimensional half-space with constant physical parameters, is given in terms of thermal inertia as

$$P^2 \frac{\delta T(x, t)}{\delta t} = k^2 \frac{\delta^2 T(x, t)}{\delta x^2}; \quad (2)$$

$T(x, t)$ is temperature at depth x and time t . Boundary conditions used by Jaeger (1953) and others are

$$\left| \lim_{x \rightarrow \infty} T(x, t) \right| < \infty \quad (2.1)$$

$$T(x, 0) = T_0 \quad (2.2)$$

$$-k \frac{\delta T(x, t)}{\delta x} \Big|_{x=0} = G(t). \quad (2.3)$$

The general Fourier series solution to [2] with the properties that T is periodic in time and exponentially decaying with depth is (Carslaw & Jaeger, 1959, p65)

$$T(x, t) = T(x, 0) + \sum_{n=1}^{\infty} A_n e^{-\frac{kx\sqrt{\omega n}}{k}} \cos\left(\omega t - \frac{P}{k} x \sqrt{\omega n} - \epsilon_n\right), \quad (3)$$

ω is the fundamental frequency, ϵ_n is the phase shift of the n th harmonic of surface temperature with respect to zero time (taken here

as solar noon), and A_n is the amplitude of the n th harmonic. Surface temperature is

$$T(0, t) = T(0, 0) + \sum_{n=1}^{\infty} A_n \cos(\omega t - \epsilon_n), \quad (3.1)$$

and periodic heating at the surface expressed as harmonic functions of ω is

$$G(t) = P \sum_{n=0}^{\infty} \sqrt{\omega n} A_n \cos\left(\omega t - \epsilon_n + \frac{\pi}{4}\right) = \sum_{n=0}^{\infty} C_n \cos(\omega t - r_n). \quad (4)$$

If $G(t)$ are known then the magnitude ($C_n = PA_n \sqrt{\omega n}$) and phase ($r_n = \epsilon_n - \frac{\pi}{4}$) quantities can be estimated using standard discrete Fourier methods on G so that P may be derived as the ratio of measured to predicted change in surface temperature between times t_1 and t_2 (Cracknell & Xue, 1996b)

$$P = \frac{\sum_{n=1}^{\infty} \frac{C_n}{\sqrt{\omega n}} \cos\left(\omega t_1 - r_n - \frac{\pi}{4}\right) - \sum_{n=1}^{\infty} \frac{C_n}{\sqrt{\omega n}} \cos\left(\omega t_2 - r_n - \frac{\pi}{4}\right)}{T_{\text{measured}}(0, t_1) - T_{\text{measured}}(0, t_2)}. \quad (5)$$

Temperature changes are used to account for the unknown initial condition, $T(0, 0)$, and a fundamental frequency of $\omega = 1$ [day⁻¹], which describes diurnal heating, leads to a daily effective value of P from [5].

2.2. The MEP model

Given limited knowledge about any system, the most likely state of the system is the one which maximizes the statistical entropy (see Shannon, 1948) of the uncertainty probability distribution (Jaynes & Bretthorst, 2003, pp 353). Wang and Bras (2011) showed that under this consideration, the maximally likely state of the land surface energy balance is the one which minimizes the dissipation function

$$D = 2 \left(\frac{G^2}{P} + \frac{H^2}{I_h} + \frac{E^2}{I_e} \right), \quad (6)$$

under the constraint

$$R = G + H + E \quad (7)$$

where R , H and E [Wm⁻²] are net radiation, sensible heat flux and latent heat flux respectively, and I_h and I_e [Jm⁻² s^{-1/2} K⁻¹] are the thermal inertia parameters related to sensible and latent heat fluxes. Wang and Bras (2009) pointed out that sensible heat flux is actually due largely to convection rather than conduction and that I_h should be interpreted as a thermal inertia-like parameter of turbulent heat transfer. Using Monin-Obukhov similarity theory (Arya, 2001), they derived I_h as

$$I_h(t) = \rho c_p \sqrt{C_1 \kappa z} \left(C_2 \frac{\kappa z g}{\rho c_p T_{\text{ref}}} \right)^{\frac{1}{6}} |H(t)|^{\frac{1}{6}} = (I) |H(t)|^{\frac{1}{6}}, \quad (8)$$

where ρ is the density of air, c_p is the specific heat capacity of air, κ is the von Karman constant, g is gravity, and C_1 and C_2 are parameters depending on the stability of the atmosphere in the surface layer with values given by Businger et al. (1971), and listed in Wang and Bras (2009); T_{ref} is a reference temperature and z is distance from the surface. We did not use these values and instead treated I , as defined by [8], and which is a daily constant parameter of the

atmosphere, as a calibration parameter. Wang and Bras (2011) derived the corresponding expression for I_e as

$$I_e(t) = \frac{\lambda^2 q_s(t)}{c_p R_v T(0, t)^2} |H(t)|^{\frac{1}{6}} = s(t) I_h(t), \quad (9)$$

where R_v is the universal gas constant, λ is latent heat of vaporization and q_s is surface specific humidity. They showed that Eq. (6) is minimized under the constraint (7) when

$$G(t) = \left(\frac{P}{I} \right) \frac{B(t)}{s(t)} H(t) |H(t)|^{-\frac{1}{6}} \quad \text{and} \quad (10.1)$$

$$E(t) = B(t) H(t); \quad (10.2)$$

$$B(t) = 6 \left(\sqrt{1 + \frac{11}{36} s(t)} - 1 \right). \quad (10.3)$$

Wang and Bras (2011) estimated P using measurements of soil moisture and, rather than calibrating T_{ref} and z in [8], calibrated I directly using observations of energy fluxes for some time period under the assumption that I was constant at a given site over a number of days. Given P and I , Eq. (10) can be solved implicitly for G and H under the constraint (7).

2.3. The coupled model

For any given daily value of I , measured diurnal surface temperature fluctuation and time series of net radiation, P can be found which solves Eq. (10) under the constraints (7) and (4). In application, this is an optimization problem and for a trial value of P , time series of G , H , and E are estimated using the MEP model and an estimator \hat{P} is derived from G using Eq. (5). P is chosen such that the difference between P and \hat{P} is minimized. The coupled MEP and soil-heat diffusion model contains four unknown quantities: P , I , G and H , and three equations: Eq. (5) and Eq. (7), and Eq. (10). Combining these equations results in a relationship between I and H which is analogous to the relationship between P and G in Eq. (4),

$$(I)\Theta(t) = \frac{B(t)}{s(t)} H(t) |H(t)|^{-\frac{1}{6}}, \quad \text{where} \quad (11)$$

$$\Theta(t) = \sum_{n=0}^{\infty} \sqrt{\omega n} A_n \cos(\omega n t - \epsilon_n + \frac{\pi}{4}) \quad (11.1)$$

is from Eq. (4). If I_h were constant over a single day and not dependent on the sensible heat flux, the MEP model would be identical to a composite 1-D diffusion system with two different homogeneous half-spaces sharing a boundary at the land surface – one with thermal inertia P and one with thermal inertia I_h (Wang & Bras, 2009). Since I_h is dependent on the boundary condition, flux partitioning at

the land surface is conceptually asymmetrical and the MEP model no longer exactly represents a diffusive system. Eq. (11) is the solution of a particular linearized approximation of a hypothetical inhomogeneous diffusion-like representation of turbulent heat transfer to the atmosphere. If we accept this approximation, it is possible to estimate the total thermal inertia of the system as

$$P + (1 + B(t)) \frac{s(t)}{B(t)} I_h = \frac{R(t)}{\Theta(t)}. \quad (12)$$

Without an additional constraint we have no information about the ratio P/I , and it is necessary to parameterize the model.

2.4. Sensitivity analysis and parameterization

An appropriate parameterization of the coupled model was chosen according to a sensitivity analysis conducted using synthetic data (Fig. 1). Synthetic net radiation (R^*) was generated using a standard top-of-the-atmosphere solar radiation curve for latitude $l = 31.3^\circ$ and day-of-year $doy = 100$ attenuated by a constant multiplicative atmospheric transmissivity factor of $C_T = 0.80$ and albedo of $\alpha = 0.15$. This was further attenuated independently with probability 0.25 at each time step by a uniformly distributed multiplicative cloud factor (c_f) on the range [0.6, 1]:

$$R^*(t) = (c_f(t))(1 - \alpha)(C_T)(1367) \left(\sin\left(\frac{lt}{180}\right) \sin(d) + \cos\left(\frac{lt}{180}\right) \cos(d) \cos(2\pi t) \right) \quad (13)$$

$$d = (0.398) \text{asin}(4.871 + 0.017(doy)) + 0.033 \sin(6.224 + 0.017(doy)) \quad (13.1)$$

$$\left. \begin{array}{l} c_f(t) \sim U[0.6, 1]; P(0.25) \\ c_f(t) = 1; P(0.75) \end{array} \right\} \quad (13.2)$$

Thermal inertia values P^* were drawn from a uniform distribution on the range [700, 2500] [$\text{Jm}^{-2} \text{s}^{-1/2} \text{K}^{-1}$] and for each sampled value of P^* , P^*/I^* was set to a number of constant values: {0.5, 1, 1.5, 2, 2.5, 3, 4, 5}. A measured time series of atmospheric specific humidity (from the field site discussed in Section 3.1) was used in lieu of surface specific humidity. I^* was derived from P^* for each P^*/I^* value and surface temperature and ground heat flux were estimated implicitly using an iterative technique of alternately deriving G^* from T^* using Eq. (10) and Eq. (7) and T^* from G^* using Eq. (3.1) and Eq. (4) until T^* and C^* converged on stable values. An initial guess of $T^*(0, t) = -10 \cos(\omega t)$ was provided. After convergence, it was always the case that P^* could be derived from $T^*(0, t_1)$, $T^*(0, t_2)$ and G^* using Eq. (5) to within 1% accuracy; surface temperature measurement times were 4:00 and 13:00.

For each resulting set of R^* and T^* , P/I was varied over the range [0.1, 5.5] and G was derived for each P/I value using Eq. (10) and Eq.

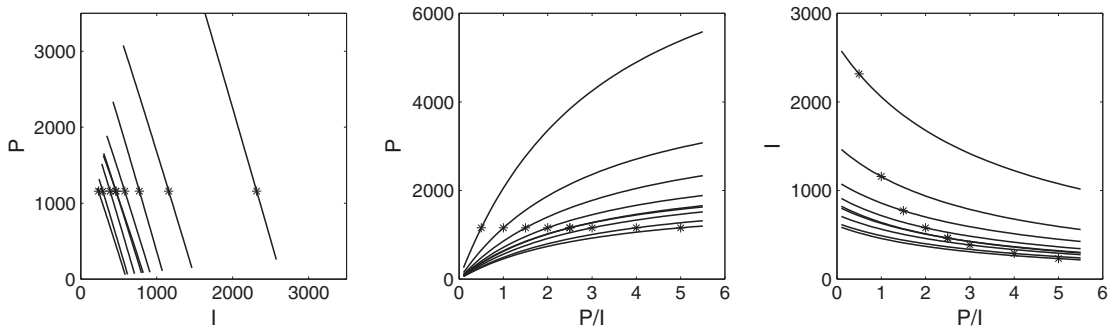


Fig. 1. Examples of theoretical relationships between model parameters P and I . The true parameters used to derive these relationships are marked with asterisks.

(7); P was derived from G and T^* using [5] and I was derived from P and P/I. Each curve in Fig. 1 represents this mutual variation of P and I (and P/I) given R^* and T^* . Results from a single value of P^* are reported; these results are representative of findings from all of the sampled P^* values. The parameters values used to generate surface temperature from net radiation for each curve (P^* , I^* and P^*/I^*) are marked with asterisks, although any point along each curve is an equally appropriate solution given the constraints of the model.

A natural extension of Wang and Bras (2011) would be to assign a constant value to I, however the sensitivity of P to I is higher than the sensitivity of P to P/I (Fig. 1) and thus it would be preferable to parameterize by P/I. The slope of relationships between I and P is much less than -1 meaning that errors in I will be magnified in estimates of P. On the other hand, relationships between P/I and P improve with larger values of P/I in the sense that errors in P/I are increasingly damped in estimates of P as P/I increases. When the coupled model is parameterized by P/I, MEP provides the boundary condition for the 1-D diffusion model and P and I are completely determined.

3. Model demonstration

In this section, we provide a demonstration of the coupled model for estimating surface fluxes, thermal inertia and soil moisture. In the following subsections we describe the study site used for this demonstration (Section 3.1), show that the constant P/I parameterization does not preclude reasonable surface flux estimates from the MEP model (Section 3.2), compare estimates of soil thermal inertia made by the coupled model to those produced by the Xue and Cracknell (1995) diffusion solution with a linearized boundary condition (Section 3.3), and derive soil moisture estimates from coupled-model thermal inertia values using the Lu et al. (2009) approach (Section 3.4). These soil moisture estimates are compared to in situ measurements. In Section 3.5 we provide a remote sensing demonstration using MODIS surface temperature measurements.

Model performance is evaluated in terms of surface flux estimates, thermal inertia estimates, and soil moisture estimates using Nash-Sutcliffe model efficiency coefficients (Nash & Sutcliffe, 1970). These statistics are identical to coefficients of determination when the linear regression between modeled and observed variables is assumed to have slope one and intercept zero. That is, when $\{y_i\}$ are the N observations, $\{\hat{y}_i\}$ are the N model predictions, and \bar{y} is the mean of the observations the model efficiency is defined as

$$r_{NS} = 1 - \frac{\sum_{i=1}^N (\hat{y}_i - y_i)^2}{\sum_{i=1}^N (y_i - \bar{y})^2}. \quad (14)$$

Model efficiency has range $r_{NS} \in (-\infty, 0]$ and larger values indicate superior models; when r_{NS} is negative, the mean of the observations provides a better predictor of $\{y_i\}$ than the model.

3.1. Study sites and data

Data used for demonstrating the model came from two measurement sites at the Walnut Gulch Experimental Watershed in southern Arizona, USA over one calendar year from Jan 1 to Dec 31, 2010. Lucky Hills (31.744°N, 110.052°W, 1370 m) is a desert shrubland site dominated by a diverse stand of mainly-Chihuahuan species (Scott et al., 2006). Kendall (31.737°N, 109.942°W, 1531 m) is a semidesert grassland site comprised mainly of C4 grasses with a few scattered shrubs (Scott et al., 2010). The soil at Lucky hills is 52% sand, 20% silt and 25% clay with 0.8% organic carbon fraction and the soil at Kendall is 55% sand, 26% silt, and 22% clay with 1.1% organic carbon fraction (Ritchie et al., 2009). Soil porosity was calculated using a pedotransfer function from Cosby et al. (1984) as $SW_s = 0.34 [m^3 m^{-3}]$ at Lucky hills and $SW_s = 0.42 [m^3 m^{-3}]$ at Kendall. Average annual rainfall is

320 mm at Lucky Hills and 340 mm at Kendall (Scott, 2010) with ~60% of the rainfall arriving around the summer months of July – September. Net radiation, surface temperature, atmospheric specific humidity, soil moisture and all surface fluxes were measured every half hour; soil moisture was measured at a depth of 5 cm below bare soil and surface temperature was measured over bare soil. Sensible and latent heat fluxes are measured using an eddy covariance tower and ground heat flux is measured with soil heat flux plate (REBS Inc., Seattle, WA) installed 8 cm below bare soil near both sites surface temperature measurement sites. Average soil temperature for 0–8 cm soil depth was determined by averaging measurements from thermocouples located at depths 2 and 5 cm above each soil heat flux plate. Measurements of the rate of change of soil temperature above the heat flux plates in combination with the soil bulk density and soil water content allowed calculation of the ground heat flux at the surface (G) by determining the changes in heat storage of the 0–8 cm soil layer (Scott, 2010). We used atmospheric specific humidity as a surrogate for surface specific humidity, which is difficult to measure. During 2010, there were 315 days without bad or missing surface flux data at Lucky Hills and 316 days at Kendall. Except when noted, we used only two measurements of surface temperature daily – one taken in the morning at 4:00 and one taken in the afternoon at 13:00 in order to capture diurnal surface temperature fluctuation.

Validation P values were computed using the 1-D diffusion model (Eq. (5)) with measured ground heat flux boundary conditions and two daily measurements of surface temperature. These values represent the best estimates of soil thermal inertia available using surface flux measurements without detailed knowledge of the subsurface. Validation I values were obtained by optimizing the coupled model with respect to I – that is, by choosing I independently each day to minimize the difference between that day's validation P value and P estimated by the coupled model. Half-hourly time series of measured specific humidity and half-hourly time series of surface temperature were used in Eq. (9) for calibrating daily validation values. Daily validation I values for 2010 had coefficients of variation $\frac{\sigma}{\mu} = 0.205$ at Lucky Hills and $\frac{\sigma}{\mu} = 0.194$ at Kendall; and daily validation P/I values had coefficients of variation $\frac{\sigma}{\mu} = 0.217$ at Lucky Hills and $\frac{\sigma}{\mu} = 0.198$ at Kendall (Fig. 2). The dispersion of these distributions were similar at each site which supports the decision to use a constant P/I rather than a constant I based on the sensitivity of P discussed in Section 2.4.

3.2. Surface flux estimates

To assess the impact of the constant annual parameterization on MEP model performance we compared estimates of surface energy fluxes made both using daily validation P and I values and using an annual constant P/I to ground-truth measurements. Ground, sensible and latent heat fluxes were estimated at a 1/2 h time step at both sites over the course of the year. In the validation parameter case, the entire half-hourly time series of surface temperature was used in Eq. (9) whereas in the constant annual parameterization case, surface temperature necessary for Eq. (9) was approximated as a diurnal sine curve with amplitude equal to the difference between twice-daily surface temperature measurements taken at 4:00 and 13:00. In the latter case, a value of $P/I = 2$ was used at both sites which was close to the mode of the validation parameter distributions (Fig. 4). As we will demonstrate, it was unnecessary to refine this parameter estimate further suggesting that a reasonable value can be sufficient. These flux estimates were compared to measured surface fluxes at Lucky Hills (Fig. 3) and Kendall (Fig. 4); model efficiency coefficients are listed in Table 1. The constant annual P/I parameterization reduced the efficiencies for various fluxes by between 2% and 9% at Lucky Hills and 0.5% to 3% at Kendall as compared to fluxes predicted using (daily) validation P and I values derived directly from half-hourly time series of measurements of ground heat flux. The

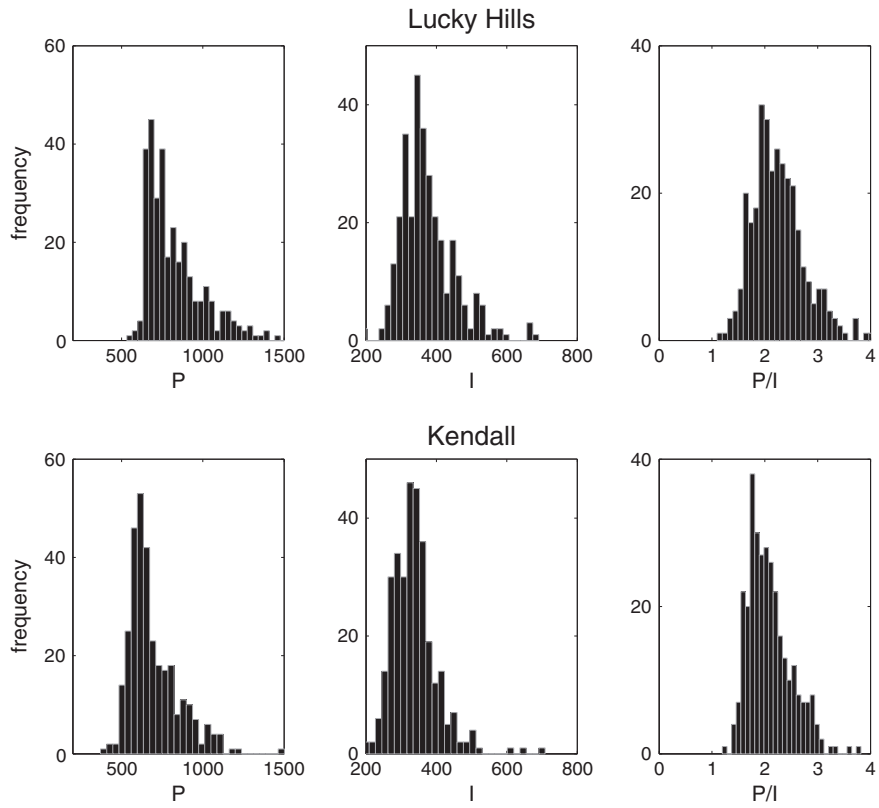


Fig. 2. Histograms of validation MEP parameter values at (top) Lucky Hills and (bottom) Kendall. The coefficient of variation of I at the two sites are Lucky Hills: $\frac{\sigma}{\mu} = 0.205$ and Kendall: $\frac{\sigma}{\mu} = 0.194$, and of P/I are Lucky Hills: $\frac{\sigma}{\mu} = 0.217$ and Kendall: $\frac{\sigma}{\mu} = 0.198$.

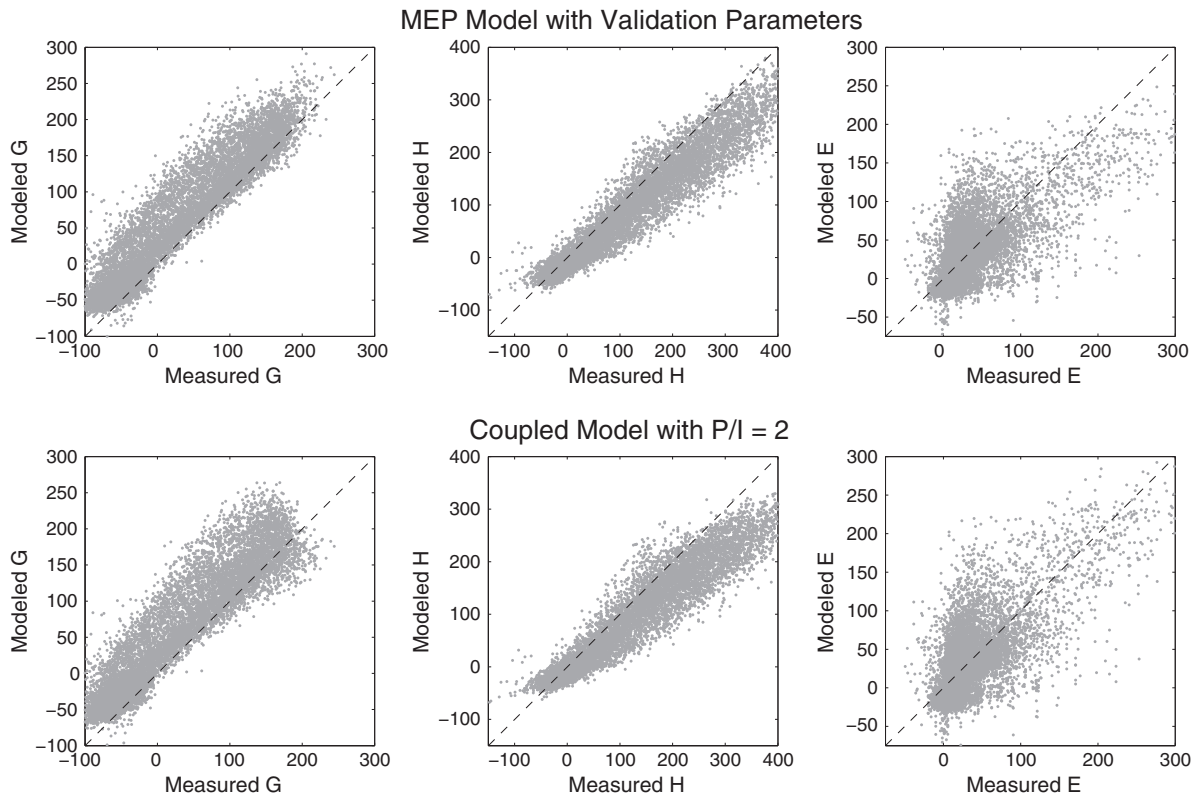


Fig. 3. Scatter plots of half-hourly flux estimates at Lucky Hills for 315 days in 2010. Efficiency coefficients are listed in Table 1.

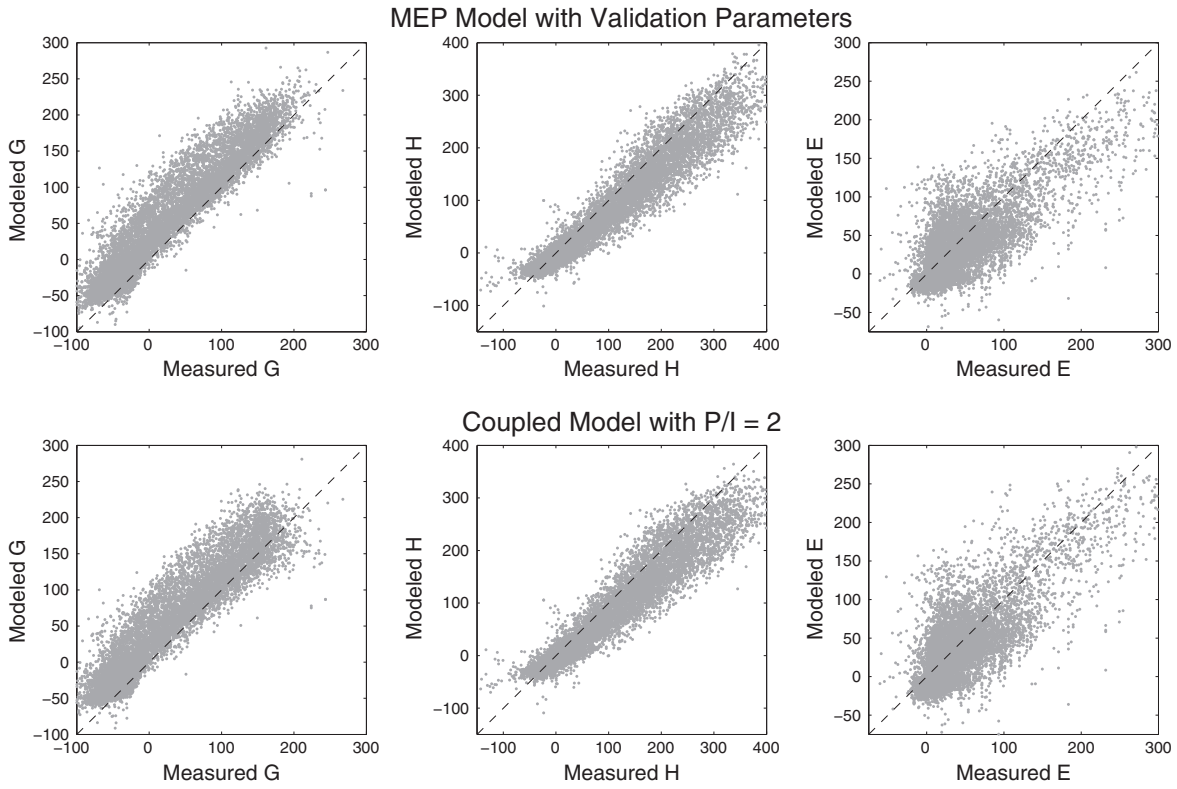


Fig. 4. Scatter plots of half-hourly flux estimates at Kendall for 316 days in 2010. Efficiency coefficients are listed in Table 1.

efficiency coefficients between flux values estimated by MEP with validation parameters and the constant parameterization were greater than $r_{NS} = 0.95$ in all cases (Table 1).

3.3. Thermal inertia estimates

When the coupled model is parameterized by P/I, it is possible to estimate P using G predicted by MEP to derive the Fourier coefficients needed for Eq. (4) – that is, MEP supplies the boundary condition needed by the diffusion model. This parameterization does not take advantage of the diffusion and MEP coupling to constrain surface flux estimates but it is the preferred coupling for predicting P given the sensitivity analysis from Section 2.4. Daily values of P and I were estimated at Lucky Hills for 315 days and Kendall for 316 days in 2010 using the coupled model and these estimates were compared to validation P and I values derived using Eq. (5) with Fourier coefficients determined from measured G time series (Fig. 5). The efficiency coefficients for P were $r_{NS} = 0.435$ at Lucky Hills and $r_{NS} = 0.587$ at Kendall. This comparison serves to validate the MEP as a boundary condition for the problem of estimating thermal inertia, but it does

not investigate the assumptions of 1-D homogeneous thermal diffusion.

As a comparison, we tested the Xue and Cracknell (1995) model of thermal inertia which is based on similar principles as [5] but uses a boundary condition which approximates H and E fluxes as a linear function of surface temperature based on the suggestion of Watson (1975). Though the original implementation uses a standard daily solar radiation curve in the boundary condition, we used net radiation to account for clouds; this resulted in an expression for ground heat flux:

$$G(t) = R(t) - A_c - BT(0, t). \tag{15}$$

A_c and B are linearization coefficients. Xue and Cracknell (1995) showed that the system Eq. (2) with boundary condition (15) can be solved for P given two daily measurements of surface temperature and an estimate of the phase difference between surface temperature and radiation; the bias A_c cancels in the same way as $T(0,0)$ by using measured daily temperature changes and the value of B is completely (implicitly) determined by the phase difference. The phase shift of radiation with respect to solar noon for harmonic n is δ_n , and the expression for diurnal temperature fluctuation is

$$T(0, t_1) - T(0, t_2) = \sum_{n=1}^{N_t} A_n \frac{\cos(\omega n t_1 - \epsilon_n) - \cos(\omega n t_2 - \epsilon_n)}{P \sqrt{\omega n + \frac{\omega \sqrt{n}}{b} + \frac{\omega}{2b^2}}} \tag{16}$$

$$b = \frac{\tan(\epsilon_1 - \delta_1)}{1 - \tan(\epsilon_1 - \delta_1)}, \tag{16.1}$$

$$\epsilon_n = \text{atan}\left(\frac{b\sqrt{n}}{1 + b\sqrt{n}}\right) + \delta_n. \tag{16.2}$$

Solving Eq. (16) for P given measurements of $T(0, t_1)$ and $T(0, t_2)$ results in an expression analogous to Eq. (5) when the boundary

Table 1 Efficiency coefficients between measurements and estimates of half-hourly surface fluxes at Lucky Hills (315 days) and Kendall (316 days) in 2010 made with the MEP model parameterized with daily validation parameters and a constant P/I = 2.

		MEP w/ validation parameters vs. measured	MEP w/ constant P/I = 2 vs. measured	MEP w/ constant P/I = 2 vs. MEP w/ validation parameters
Lucky hills	G	0.786	0.760	0.973
	H	0.886	0.866	0.991
	E	0.500	0.455	0.967
Kendall	G	0.783	0.778	0.980
	H	0.910	0.899	0.994
	E	0.623	0.604	0.975

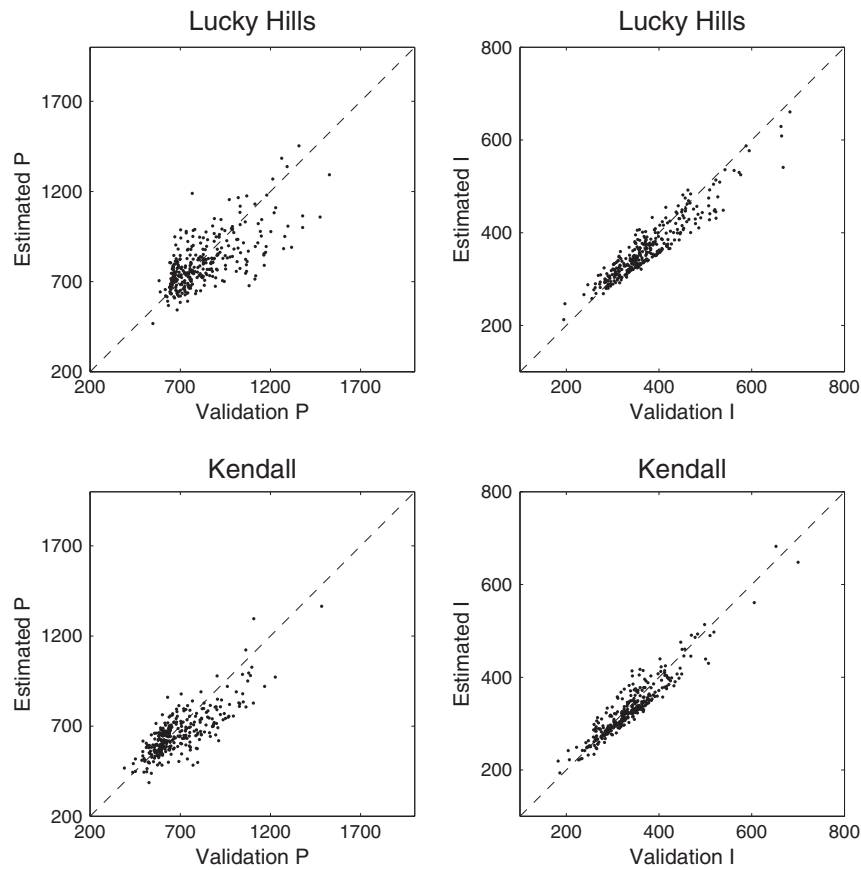


Fig. 5. Scatter plots of daily P and I estimates made using the coupled model with $P/I=2$ plotted against validation daily P and I values calculated using measured G to derive Fourier coefficients for equation [4]. Lucky Hills (top) uses 315 days worth of data from 2010 and Kendall (bottom) uses 316 days. Efficiency coefficients for P estimates at the two sites are Lucky Hills: $r_{NS} = 0.435$ and Kendall: $r_{NS} = 0.587$.

condition is Eq. (15) rather than a measured or directly estimated G time series. In a situation where net radiation cannot be approximated by a single harmonic, it is necessary to calculate all of the δ_n directly from the net radiation time series using standard Fourier methods, and also to calculate ϵ_1 from the full daily temperature time series. We used the entire day's temperature time series to find the phase difference between the first harmonic of radiation and temperature, $(\epsilon_1 - \delta_1)$, which is used in Eqs. (16) and (1), and estimate P as the ratio of modeled to measured surface temperature in a

way analogous to Eq. (5) using Eq. (16) to model diurnal surface temperature fluctuations. This model utilizes the entire day's time series of surface temperature whereas our implementation of the coupled MEP-diffusion model only utilizes surface temperature measurements at two time points. These estimates of P were compared to validation values (Fig. 6) and have efficiency coefficients $r_{NS} = -12.3$ at Lucky Hills and $r_{NS} = -6.81$ at Kendall compared to $r_{NS} = 0.435$ at Lucky Hills and $r_{NS} = 0.587$ at Kendall using the MEP boundary condition.

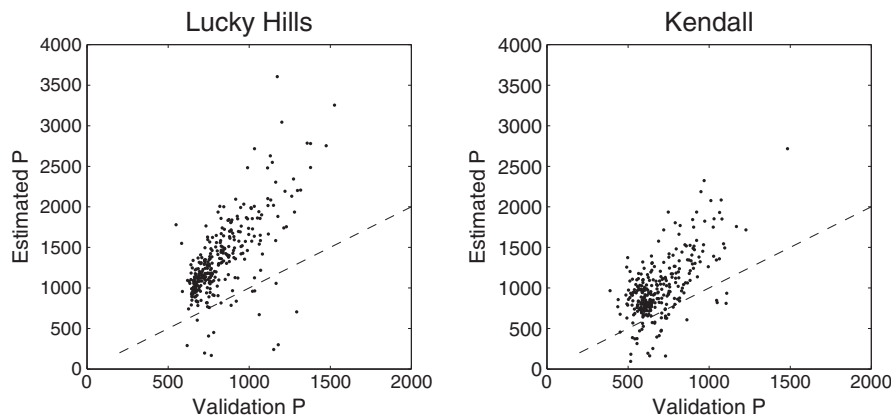


Fig. 6. Scatter plots of daily P estimates made using the Xue and Cracknell model with a linearized boundary condition plotted against validation P values. Efficiency coefficients are Lucky Hills: $r_{NS} = -12.3$ and Kendall: $r_{NS} = -6.14$.

3.4. Soil moisture estimates

Our motivation for estimating thermal inertia was ultimately to exploit its dependence on water content in order to estimate soil moisture. Lu et al. (2009) described a model relating volumetric soil water content (SW [m^3m^{-3}]) to thermal inertia based on the original theory of de Vries (1963):

$$SW = M_f(SW_s - SW_r) + SW_r \quad (17)$$

$$M_f = \left(1 - \frac{\ln\left(\frac{P - P_r}{P_s - P_r}\right)}{\varepsilon}\right)^{-\frac{1}{\mu}} \quad (17.1)$$

$$P_r = -1.0624(SW_s) + 1.0108 \quad (17.2)$$

$$P_s = \sqrt{k_s c_s} \quad (17.3)$$

$$c_s = \rho_q c_q (1 - SW_s) + \rho_w c_w n \quad (17.4)$$

$$k_s = \left(\left(k_q^{s_f}\right)\left(3^{1-s_f}\right)\right)^{1-n} (k_w)^n \quad (17.5)$$

Physical constants are: specific heat capacity of water $c_w = 4.18$ [$\text{Jm}^{-3}\text{K}^{-1}$], specific heat capacity of quartz $c_q = 0.80$ [$\text{Jm}^{-3}\text{K}^{-1}$], thermal conductivity of water $k_w = 0.594$ [$\text{Wm}^{-1}\text{K}^{-1}$], thermal conductivity of quartz $k_q = 7.7$ [$\text{Wm}^{-1}\text{K}^{-1}$], density of water $\rho_w = 1$ [g cm^{-3}], and quartz density $\rho_q = 2.65$ [g cm^{-3}]. M_f is the moisture fraction (between residual and porosity), P_s is the thermal inertia of saturated soil and P_r is the thermal inertia of soil at residual moisture content. Free parameters are: sand fraction s_f [m^3m^{-3}], organic matter fraction o_f [m^3m^{-3}], porosity SW_s [m^3m^{-3}], residual water content SW_r [m^3m^{-3}], and two empirical shape parameters ε and μ . We set the sand and organic matter fractions according to Ritchie et al. (2009) and porosity according to Cosby et al. (1984) (Section 3.1) and used a daily mean value of measured SW and daily validation P values to calibrate the residual moisture content and shape parameters ε and μ by hand; the resulting model is compared to calibration data (validation P and measured soil moisture) in Fig. 7, and the calibrated parameter values are listed in Table 2. Negative errors in P estimates for soil with low moisture content can result in thermal inertia values which are less than the residual moisture thermal inertia value (P_r); when this occurred we set the estimated soil moisture value to residual moisture content ($SW = SW_r$).

We used the calibrated model to predict daily soil moisture at Kendall and Lucky hills using estimates of thermal inertia from the coupled MEP and diffusion model (Fig. 8). At low soil moisture values

Table 2

Parameters for the Lu et al. (2009) model [17] to estimate soil moisture from thermal inertia at Lucky Hills and Kendall. Sand fraction and organic matter fraction are from (Ritchie et al., 2009).

	Sand Fraction [m^3m^{-3}]	Organic Fraction [m^3m^{-3}]	Porosity [m^3m^{-3}]	Residual Water Content [m^3m^{-3}]		
Lucky Hills	0.52	0.01	0.34	0.04	0.40	2.65
Kendall	0.55	0.01	0.42	0.03	0.65	2.95

(~ 0.1 [m^3m^{-3}]) there is almost no expected change in thermal inertia with change in moisture (Fig. 7), meaning that small errors in P resulted in large errors in SW when the soil was dry. At higher moisture levels, thermal inertia was more sensitive to changes in soil water content and predictions became more accurate in wetter conditions. This was due to the fact that soil at the Walnut Gulch were relatively dry for most of the year, and at very low moisture contents, soil water exists as an absorbed film and does not span gaps between solid soil particles. Until a critical moisture value is reached (dependent on clay content and particle size) thermal conductivity and thermal inertia are insensitive to moisture content (Tarnawski & Leong, 2000). The relationships between thermal inertia and soil moisture which we saw at the Kendall and Lucky Hills sites were conceptually similar to those found in fine-grained soils such as reported by Murray and Verhoef (2007) (see their Fig. 1b), although the critical values at our study sites were higher than in previously-reported soils. These high critical values were likely due to high gravel content in the topmost soil layer at these study sites. The efficiency coefficients for these SW estimates were both less than zero: $r_{NS} = -0.184$ at Lucky Hills and $r_{NS} = -0.052$ at Kendall. This inefficiency was due largely to the high critical value and the sensitivity of thermal inertia to soil moisture content.

3.5. MODIS demonstration

We used the new method for estimating thermal inertia with MODIS surface temperature data derived from Aqua images of the Walnut Gulch watershed (~ 150 km^2) taken in July and August of 2004. Soil moisture (5 cm depth), net radiation and specific humidity were measured at both Lucky Hills and Kendall during this time period. Before July 13 (doy 195), the soil at Lucky Hills was very dry ($SW \sim 0.03$ [m^3m^{-3}]) and slightly wetter ($SW \sim 0.08$ [m^3m^{-3}]) at Kendall. Between July 13 and Aug 24 (doy 237) there was approximately 95[mm] of measured precipitation. We estimated thermal inertia from 21 day and night Aqua image pairs acquired from the Land Process Distributed Active archive Center (LP-DAAC, 2007) and re-

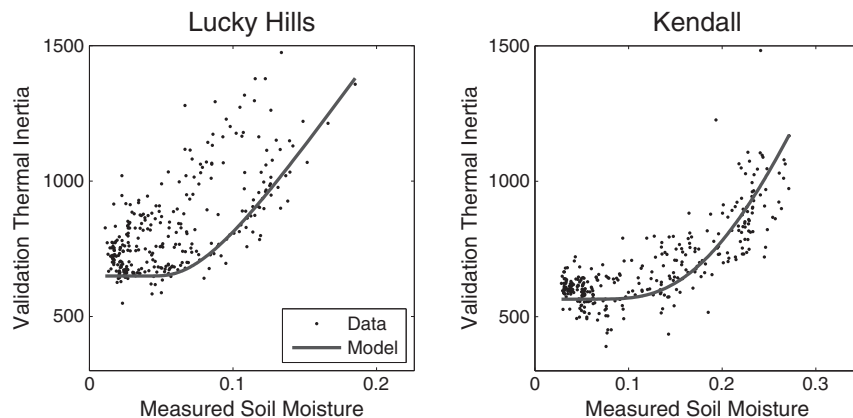


Fig. 7. The relationship between validation thermal inertia and soil moisture according to [17] with parameters from Table 2 (solid line) and estimates of thermal inertia from the coupled MEP-diffusion model and daily-averaged soil moisture (scatter points) at Lucky Hills and Kendall.

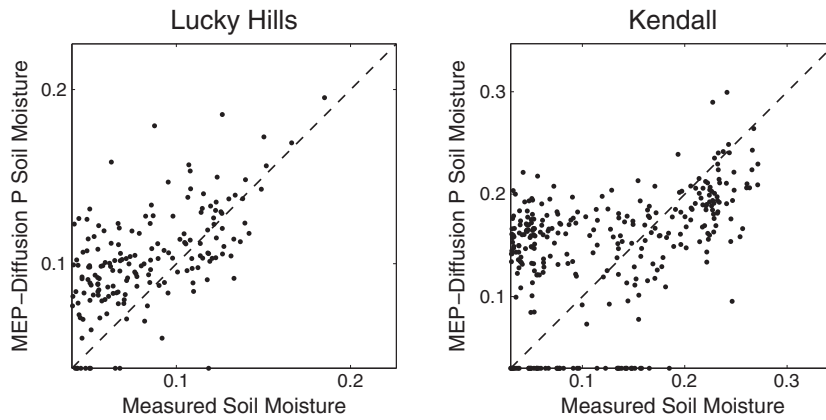


Fig. 8. Scatter plots of daily soil moisture estimates made using P from the coupled model plotted against measured daily average soil moisture values at Lucky Hills (top) and Kendall (bottom). Efficiency coefficients for these soil moisture estimates are Lucky Hills: $r_{NS} = -0.184$ and Kendall: $r_{NS} = -0.052$.

sampled onto a NAD83 projection grid; the spatial resolution of these images before and after reprojection was ~ 0.927 [km]. Night overpass times ranged from 1:00 to 3:00 and day overpass times ranged from 12:00 to 14:00; overpass times were approximated to the nearest hour. Hourly net radiation and specific humidity time series at each image pixel for each day were extrapolated as inverse-distance weighted combinations (linear) of measurements taken at Kendall and Lucky Hills, and thermal inertia was calculated by the coupled model as described in Section 2 with $P/I=2$.

Thermal inertia images from day 186, 233 and 238, are illustrated in Fig. 9; lighter pixel color corresponds to higher thermal inertia and wetter soil. Approximately 90[mm] of precipitation fell between day 186 and day 233, and 3–5[mm] fell on day 237. These images indicate that the soil was generally wetting between day 186 and day 233 and

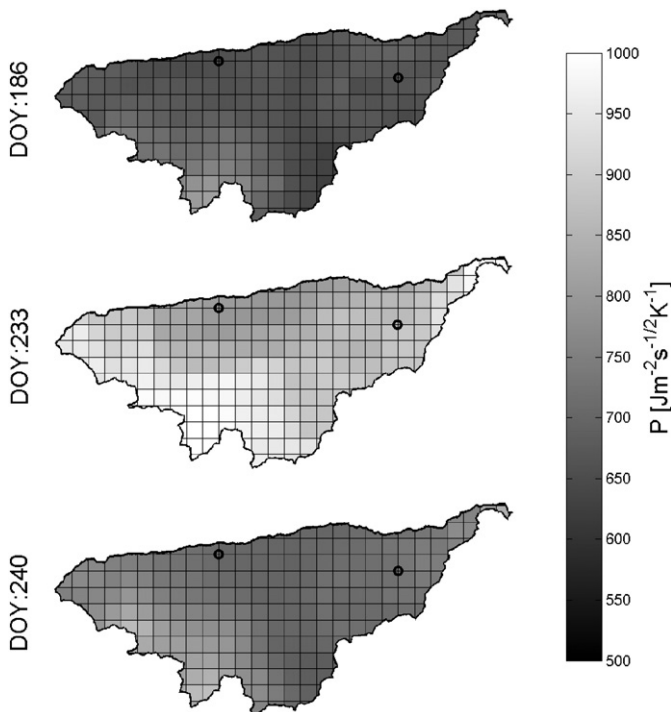


Fig. 9. Thermal inertia maps derived from three level 3 MODIS Aqua day and night image pairs with spatial resolution ~ 0.927 [km]. The Walnut Gulch watershed is outlined and data points which are closest to the Kendall (East) and Lucky Hills (West) measurement stations are marked. Soil moisture on these dates was, at Kendall: 0.07, 0.12, and 0.10 [$\text{m}^3 \text{m}^{-3}$], and at Lucky Hills: 0.03, 0.10, and 0.09 [$\text{m}^3 \text{m}^{-3}$] on days of year 186, 233, and 238 respectively.

drying between day 233 and day 238. At Lucky Hills, except for in very dry conditions ($SW=0.03$ [$\text{m}^3 \text{m}^{-3}$]) MODIS-derived thermal inertia was strongly related to measured water content. Fig. 10 plots this relationship along with a Lu model, [17], with shape coefficients calibrated to this data ($\mu=0.60$ and $\varepsilon=1.00$). The MODIS measured thermal inertia was often less than P_r approximated by [17,2], and it was necessary to assign a value of $P_r=400$ [$\text{Jm}^{-2} \text{s}^{-1/2} \text{K}^{-1}$]. At Kendall, which is a grassland site, the correlation between thermal inertia and measured soil moisture (not shown) was negative due to the fact that evapotranspiration during the daytime was higher when there was moisture available in the near-surface soil. Higher evapotranspiration caused surface cooling from the perspective of the satellite, and there were smaller diurnal surface temperature fluctuations when water was available for transpiration by C4 grasses.

4. Conclusions and discussion

Results showed that it is possible to estimate soil thermal inertia from net radiation specific humidity and two daily measurements of surface temperature by coupling the recently developed MEP model of surface energy fluxes with the classical diffusion model of ground heat flux. This coupling approximates sensible and latent heat transfer to the atmosphere as a linear diffusive system even though the thermal inertia of the air is taken to be dependent on the sensible heat flux. The coupling reduces the number of free system parameters from two to one – P is determined uniquely by the choice of I, – and

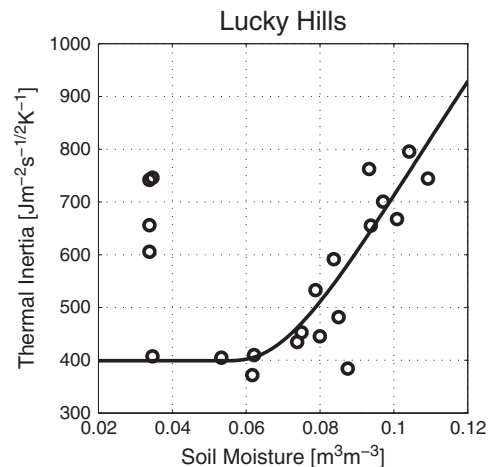


Fig. 10. Relationship between MODIS-derived thermal inertia and daily soil moisture measured at Lucky Hills plotted against a calibrated Lu model with shape coefficients: $\mu=0.60$ and $\varepsilon=1.00$.

we demonstrated that when estimating P, it is preferable to parameterize by a constant P/I rather than a constant I as had been done previously. We demonstrated the model at two field sites where this parameterization was appropriate and where it was reasonable to choose a constant P/I for an entire calendar year.

Results showed that:

- (i) The MEP model parameterized by an annually constant P/I predicted surface fluxes with accuracy similar to the MEP model parameterized by daily P and I calibrated directly from measured ground heat flux and surface temperature assuming 1-D homogeneous diffusion in the subsurface;
- (ii) The coupled model produced estimates of soil thermal inertia which were superior to those produced by the Xue and Cracknell diffusion solution with a linearized boundary condition; and
- (iii) Thermal inertia was not sensitive to soil moisture at low moisture contents, however the relationship improved in moderately wet conditions.

There are still several issues with the application of this method which will need to be addressed before it can be expected to estimate soil moisture in an operational remote sensing setting. First, it is not reasonable to expect to have time series of net radiation and specific humidity measured at a sub-daily time step at the arbitrary location. It might, however, be possible to constrain a spatially distributed set of model solutions, over, for instance, a pixelated thermal image, by making assumptions about homogeneous cloud cover. Second, the model is only applicable to bare soil conditions given that the temperature of the soil surface must be known in order to apply the ground heat flux boundary condition. The MEP is theoretically able to predict evapotranspiration and it might be possible to estimate soil surface temperature by considering the extent of vegetation cover and the magnitude of the evapotranspiration flux. The implications of this or another type of approximation will need to be assessed. Third, the parameterization by P/I is sub-optimal. It would be desirable to constrain this value at the daily time scale using additional information, either in the form of an independent measurement or an independent relationship between P and I or G and H; many such relationships have been proposed which could be examined for application to this problem. Finally, the estimation of soil moisture using the Lu et al. (2009) model requires a set of parameters (s_f , O_f , SW_s , SW_r , ϵ and μ) which we cannot expect to calibrate at an arbitrary remote sensing location. A holistic approach to addressing these concerns might be to use a dynamic model of soil moisture in conjunction with the MEP boundary condition to estimate P. Soil moisture accounting, in part driven by MEP estimates of latent heat flux, would provide an uncertain constraint on daily values of P given uncertainties in parameterization, vegetation and clouds.

Acknowledgments

This work was supported by NASA grant 08-SMAPSDT08-0042 affiliated with the SMAP (Soil Moisture Active-Passive) mission Science Definition Team (PI – M.S. Moran). The authors would like to thank Jingfeng Wang at the Department of Civil and Environmental Engineering, University of California Irvine for his assistance with the MEP model. MODIS data were obtained through the online Data Pool at the NASA Land Processes Distributed Active Archive Center

(LP DAAC), USGS/Earth Resources Observation and Science (EROS) Center, Sioux Falls, South Dakota (http://lpdaac.usgs.gov/get_data).

References

- Arya, S. P. (2001). *Introduction to Micrometeorology*. London, UK: Academic Press.
- Businger, J. A., Wyngaard, J. C., Izumi, Y., & Bradley, E. F. (1971). Flux-profile relationships in the atmospheric surface layer. *Journal of the Atmospheric Sciences*, 28, 181–189.
- Carlsaw, H. S., & Jaeger, J. C. (1959). *Conduction of heat in solids*. Oxford, UK: Clarendon Press.
- Cosby, B. J., Hornberger, G. M., Clapp, R. B., & Ginn, T. R. (1984). A statistical exploration of the relationships of soil moisture characteristics to the physical properties of soils. *Water Resources Research*, 20, 682–690.
- Cracknell, A. P., & Xue, Y. (1996). Dynamic aspects study of surface temperature from remotely-sensed data using advanced thermal inertia model. *International Journal of Remote Sensing*, 17, 2517–2532.
- Cracknell, A. P., & Xue, Y. (1996). Thermal inertia determination from space – a tutorial review. *International Journal of Remote Sensing*, 17, 431–461.
- de Vries, D. A. (1963). Thermal properties of soils. In W. R. Wijk (Ed.), *Physics of Plant Environment* (pp. 210–235). Amsterdam, The Netherlands: North-Holland Publishing Company.
- Dewar, R. (2005). Maximum entropy production and the fluctuation theorem. *Journal of Physics a-Mathematical and General*, 38, L371–L381.
- Jaeger, J. C. (1953). Conduction of heat in a solid with periodic boundary conditions, with an application to the surface temperature of the moon. *Proceedings of the Cambridge Philosophical Society*, 49, 355–359.
- Jaynes, E. T., & Bretthorst, G. L. (2003). *Probability Theory: The Logic of Science*. New York: Cambridge University Press.
- LP-DACC: NASA Land Processes Distributed Active Archive Center (2007). *MODIS/Aqua Land Surface Temperature and Emissivity Daily L3 Global 1 km Grid SIN (MYD11A1), Version 005*. Sioux Falls, South Dakota: USGS/Earth Resources Observation and Science (EROS) Center.
- Lu, S., Ju, Z. Q., Ren, T. S., & Horton, R. (2009). A general approach to estimate soil water content from thermal inertia. *Agricultural and Forest Meteorology*, 149, 1693–1698.
- Murray, T., & Verhoef, A. (2007). Moving towards a more mechanistic approach in the determination of soil heat flux from remote measurements – I. A universal approach to calculate thermal inertia. *Agricultural and Forest Meteorology*, 147, 80–87.
- Nash, J. E., & Sutcliffe, J. V. (1970). River flow forecasting through conceptual models part I – a discussion of principles. *Journal of Hydrology*, 10, 282–290.
- Price, J. C. (1980). The potential of remotely sensed thermal infrared data to infer surface soil-moisture and evaporation. *Water Resources Research*, 16, 787–795.
- Ritchie, J. C., Nearing, M. A., & Rhoton, F. E. (2009). Sediment budgets and source determinations using fallout Cesium-137 in a semiarid rangeland watershed, Arizona, USA. *Journal of Environmental Radioactivity*, 100, 637–643.
- Scott, R. L. (2010). Using watershed water balance to evaluate the accuracy of eddy covariance evaporation measurements for three semiarid ecosystems. *Agricultural and Forest Meteorology*, 150, 219–225.
- Scott, R. L., Hamerlynck, E. P., Jenerette, G. D., Moran, M. S., & Barron-Gafford, G. A. (2010). Carbon dioxide exchange in a semidesert grassland through drought-induced vegetation change. *Journal of Geophysical Research-Biogeosciences*, 115, G03026.
- Scott, R. L., Huxman, T. E., Cable, W. L., & Emmerich, W. E. (2006). Partitioning of evapotranspiration and its relation to carbon dioxide exchange in a Chihuahuan Desert shrubland. *Hydrological Processes*, 20, 3227–3243.
- Shannon, C. E. (1948). A mathematical theory of communication. *Bell System Technical Journal*, 27, 379–423.
- Tarnawski, V. R., & Leong, W. H. (2000). Thermal conductivity of soils at very low moisture content and moderate temperatures. *Transport in Porous Media*, 41, 137–147.
- van de Griend, A. A., Camillo, P. J., & Gurney, R. J. (1985). Discrimination of soil physical parameters, thermal inertia, and soil-moisture from diurnal surface-temperature fluctuations. *Water Resources Research*, 21, 997–1009.
- Verhoef, A. (2004). Remote estimation of thermal inertia and soil heat flux for bare soil. *Agricultural and Forest Meteorology*, 123, 221–236.
- Wang, J., & Bras, R. L. (2009). A model of surface heat fluxes based on the theory of maximum entropy production. *Water Resources Research*, 45, W11422.
- Wang, J. F., & Bras, R. L. (2011). A model of evapotranspiration based on the theory of maximum entropy production. *Water Resources Research*, 47, W03521.
- Wang, J., Bras, R. L., Sivandran, G., & Knox, R. G. (2010). A simple method for the estimation of thermal inertia. *Geophysical Research Letters*, 37, L05404.
- Watson, K. (1975). Geologic applications of thermal infrared images. *Proceedings of the IEEE*, 63, 128–137.
- Xue, Y., & Cracknell, A. P. (1995). Advanced thermal inertia modeling. *International Journal of Remote Sensing*, 16, 431–446.